

**MOLECULAR DOCKING AND ADMET STUDIES OF AMINO-PYRIMIDINE
DERIVATIVES AS MYCOBACTERIUM TUBERCULOSIS SER/THR PROTEIN
KINASES B INHIBITORS**

S. Khamouli¹, S. Belaidi^{1*}, T. Lanez²

¹Group of Computational and Medicinal Chemistry, Laboratory of Molecular Chemistry and environment, Department of Chemistry, University of Biskra, BP 145 Biskra 07000, Algeria

²VTRS Laboratory, Faculty of Sciences and Technology, University of El Oued, B.P.789, 39000 El Oued, Algeria

Received: 11 March 2019 / Accepted: 29 April 2019 / Published online: 01 May 2019

ABSTRACT

We used the molecular docking method with Molegro software and we calculate ADME-T properties using Marvin Sketch and preADMET. The 29 amino-pyrimidines ligands were examined for docking studies with PknB (PDB Code: 2FUM). The Moldock score of the best three ligands L9, L12 and L21 are -161.475, -152.003 and -143.359 Kcal/Mol. These percentage shows that these candidature ligands have high binding energy percentage than the native MIX ligand. The ligand L21 has the human intestinal absorption (HIA), Caco-2 cell permeability, and plasma protein binding values of 85.48, 6.312 (nm/Sec.) and 93.097% respectively, which are comparable to MIX and the other ligands L9, L12. This computational study helped to prove that the ligand L21 have the ability to kill the Mycobacterium tuberculosis by inhibiting the expression of protein kinase B.

Keywords: Amino-pyrimidine, Tuberculosis, PknB, Molecular docking, ADMET.

Author Correspondence, e-mail: prof.belaidi@mail.com

doi: <http://dx.doi.org/10.4314/jfas.v11i2.24>



1. INTRODUCTION

Tuberculosis is the primary cause of mortality due to an infectious disease in the world today. The causative agent of tuberculosis is the intracellular pathogen *M.tuberculosis* [1]. Recent studies have axed on finding new pathways vulnerable to inhibition by small molecules and previously unexploited by drug design efforts [2]. The inhibition of signaling pathways both in *M. tuberculosis* and the host may yield new classes of drug targets as many of recent studies are focused on developing this further [3].The emergence of multidrug-resistance strains of *Mycobacterium tuberculosis* has increased efforts to discover novel drugs for tuberculosis treatment. Targeting the persistent state of *Mycobacterium tuberculosis*, to conventional drug therapies, is of particular interest [4].

We sought to find inhibitors of an essential *M. tuberculosis* serine/threonine protein kinase; PknB is one of the most important serine/threonine protein kinases for *Mycobacterium tuberculosis* (TB) [5, 6]. The intracellular domain of PknB has the main activity of the holoenzyme, and is able to autophosphorylate and combine with ATP and its analogues [7-10]. PknB plays an important part in the growth of TB, and is necessary for survival of TB [11-13]. Change of expression index or phosphorylation of PknB can give to alteration of growth rate and morphology of TB, due to the defects in cell wall synthesis and cell division [14-16]. Because of the differences between PknB and the human protein kinases, it is widely accepted as the drug target for anti-TB. To date, several PknB inhibitors have been reported, and some of them have shown certain degree of anti-TB capability. Most of these compounds are aminopyrimidines, aminoguanidines and anthraquinones [17-22].

Computer aided method is a first approach to screening novel therapeutic agents and the discipline is an emerging strategy as it reduces many complexities of drug design process. The study of receptor-ligand interaction is a fundamental concept of rational drug design and the prediction of such interactions by molecular docking has increasing importance in the field of structure based drug discovery [23].The screening of lead molecule with good therapeutic properties and drug likeness is a tedious task in drug discovery process. Computer aided method is an easy platform to search such kinds of biologically active compounds with favorable ADMET (Absorption, Distribution, Metabolism, Excretion and Toxicity).

Molecular modeling of the amino-pyrimidine compounds based on their interactions with *Mycobacterium tuberculosis* PknB, using Molecular docking to determine the best ligands conformation when bound to the active site [24].

Finally *in silico*, ADMET studies were performed on the best ligands to compare the computed ADMET descriptor values with the accepted ranges.

2. MATERIAL AND METHODS

Protein Preparation Structure

The downloading of serine/threonine protein kinases for *Mycobacterium tuberculosis* PknB was made from the data base Brookhaven Protein Data Bank (www.rcsb.org/pdb) [25] (access code 2FUM) [26]. It is co-crystallized with inhibitors Mitoxantrone, 1, 4-Dihydroxy-5,8-bis (2-[(2-Hydroxyethyl) Amino]Ethyl}Amino)Anthra-9,10-Quinone(three-letter code: MIX). All the heteroatom's and coordinates are removed from the PDB file. The three-dimensional structure of 2FUM was obtained by X-ray diffraction in complex with a selective inhibitor Mitoxantrone with EC Number: 2.7.11.1 chains (A, B, C, D), resolution 2.89 Å, and R-value 0.218. In this study we have taken a chain A, 263 residues and 1994 atoms. This allowed us to obtain the model shown in (Figure 1).

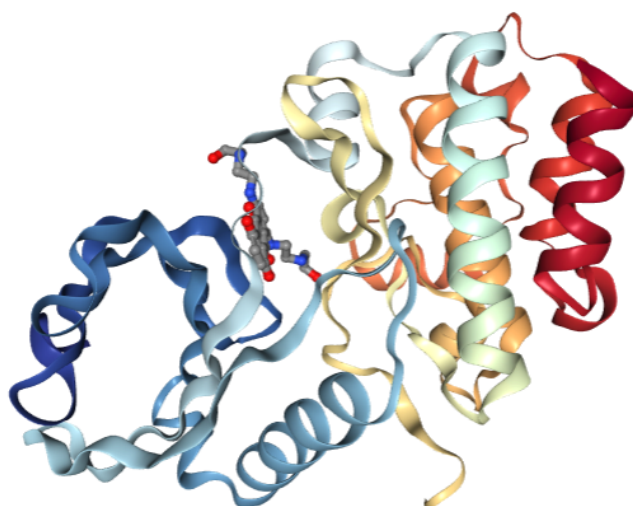


Fig.1. Three-dimensional crystal structure of the target protein

Ramachandran Plot

In this study, the stereo chemical quality of the predicted best model was validated using Rampage [27].

Ligands structure optimization

Screened of 29 amino-pyrimidine derivatives as Mycobacterium tuberculosis PknB inhibitors was selected from the literature [3,17,28], were optimized before docking using MM+ force-field (rms = 0.01 Kcal/Å) and the semi-empirical PM3 method, both of which are implemented in HyperChem 8.08 software [29]. The resulting structures were saved in “.mol” file formats for molecular docking studies.

The ligand structures of 29 amino-pyrimidine derivatives (Table1) were made by Marvin Sketch17.1.2 software [30].

Molecular Docking

Molegro Virtual Docker (MVD2012) software [31], is advanced docking analysis software used to predict protein-ligand interactions. The potential binding site of the target protein and lead candidates are identified by a molecular docking algorithm called Mol Dock, MVD works on the basis of MolDock SE search algorithm. The docking algorithm was set at a maximum iteration of 1500 with a simple evolution size of 50 and minimum of 5 runs. The population size was set at 50 with energy threshold of 100 at each step. The least minute was set as 10 minutes, the torsions/translations/rotations of the ligand-protein interaction were tested and the one giving lower energies is chosen for further studies. The bond flexibility of the ligands was fixed, and the side chain flexibility of the amino acids in the binding cavity was set with a tolerance of 1.10 and strength of 0.90 for docking simulations. Root-mean-square deviation threshold for multiple cluster poses was set at < 2.00.

Different docking programs available and they differ in the nature of the sampling algorithms they employ, in their manner of handling ligand and protein flexibility, in the scoring functions and in the CPU time they required. In the studies reported here, MVD was used, because it showed higher docking accuracy when benchmarked against other available docking programs.

(MD: 87%, Glide: 82%, Surflex: 75%, FlexX: 58%) have been shown to be successful in

several recent studies, but also for reasons of cost and user friendliness.

Binding affinities were estimated using Molegro data Modeler. The scoring function used by MolDock is derived from the piecewise linear potential scoring functions which further improves this score with a new H-bonding term and new charge schemes, being flexible, i.e. all non-ring torsions were allowed [32,33].

This molecular docking protocol generate five best predicted poses for each amino-pyrimidine compound with Moldock score, Rerank score, and Hydrogen bond score. The docked conformations or pose with the minimum MolDock score values is the optimal pose.

The docked conformation further analyzed on the basis of the Re-Rank score function. The Re-Ranking score function is generally more reliable than the MolDock score function at selecting the best solution among multiple solutions derived from the same ligand [34]. Ligplot plus 1.4.5 [35], a program to generate schematic diagrams of protein ligand interactions.

Physicochemical properties of selected ligands

Physicochemical properties of interest included predicted lipophilicity ($\log P$), predicted aqueous solubility ($\log S$), topological polar surface area (TPSA), molecular weight (MW), hydrogen bond donor (HBD), hydrogen bond acceptor (HBA), value predicted by Marvin Sketch. The calculation of partition coefficient was conducted by applying both consensus and ChemAxon methods as implemented in Marvin Sketch.

Drug Likeness and Pharmacokinetic Properties of selected ligands

The ligands were predicted for drug likeness, ADMET (adsorption, distribution, metabolism, excretion and toxicity studies by PreADMET [36]. The main filters used for prediction of drug likeliness were Lipinski's rule of five [37], CMC [38], MDDR [37], Lead-like Rule [39], and WDI (World drug index)-like rule [40]. These rules were scrutinized and were subjected to ADME prediction.

The pharmacokinetic parameters, absorption and distribution, were considered for selection of compounds as drug candidates. In this study, the PreADMET program was used to predict ADMET of amino-pyrimidine derivatives. The aspect prediction of absorption properties included percentage human intestinal absorption (% HIA) and Caco2 (heterogeneous human

epithelial colorectal adenocarcinoma), and MDCK, and MDCK (Madin-Darby canine kidney) cell permeability [41]. And blood brain barrier prediction [42]. Those molecules qualified the above rules based on specific statistical cut-off available for each model was selected for toxicity prediction. However, virtual screening was also performed to evaluate toxicological properties including carcinogenicity and risk of inhibition of human ether-a-go-go-related (hERG) gene [36]. These works have been performed by using Windows 7 64-bit operating system having Intel core 2 duo processor.

3. RESULTS AND DISCUSSION

Validation of Modeled structures

The stereo chemical quality of the predicted model was evaluated after the refinement process using Ramachandran Map calculations computed with the Procheck. The phi and psi distribution of the Ramachandran Map generated by non glycine and non proline residues are depicted in (Figure 2). Ramachandran plot indicated that no residues have phi/psi angles in the disallowed regions and hence the quality of the model is acceptable. The percentage of residues in the “core” region of our modeled protein was found to be satisfactory [43].

The red regions in the graph indicate the most allowed regions whereas the yellow regions represent allowed regions. In this protein model, 86.6% of the residues were in the most favored region, 10.9% in allowed region, 1.8 % in generously allowed region and 0.8% of the residues lying in the disallowed regions.

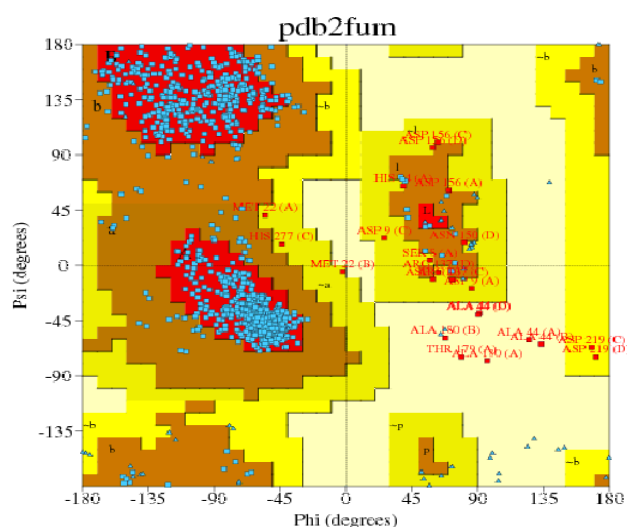


Fig.2. Ramachandran plot for 2FUM protein generated by Procheck

Prediction of binding sites

MVD automatically identifies potential binding sites (also referred as cavities or active sites) by using its cavity detection algorithm. The cavities within a $30 \times 30 \times 30 \text{ \AA}^3$ cube centered at the experimentally known ligand position were used. In the case of the crystal structures for serine/threonine protein kinase B (2FUM) complexes, the program generally identified five different binding sites (Figure 3). From these five predicted cavities (Table 1) the one with the highest volume (107.52 \AA^3) and surface (295.69 \AA^2), was selected for consideration, as it includes the bound ligand.

Table 1. Cavity information of enzyme (2FUM.pdb)

| Cavity Name | Volume(\AA^3) | Surface Area(\AA^2) |
|-------------|--------------------------|--------------------------------|
| Cavity 1 | 107.52 | 295.69 |
| Cavity 2 | 59.392 | 170.24 |
| Cavity 3 | 23.040 | 96 |
| Cavity 4 | 16896 | 80.64 |
| Cavity 5 | 16.384 | 70.4 |

The binding site was defined as a spherical region which encompasses all protein atoms within 6.0 \AA of bound crystallographic ligand atom (dimensions X (61.79 \AA), Y (2.44 \AA), Z (-25.10 \AA) axes, respectively). Default settings were used for all the calculations.

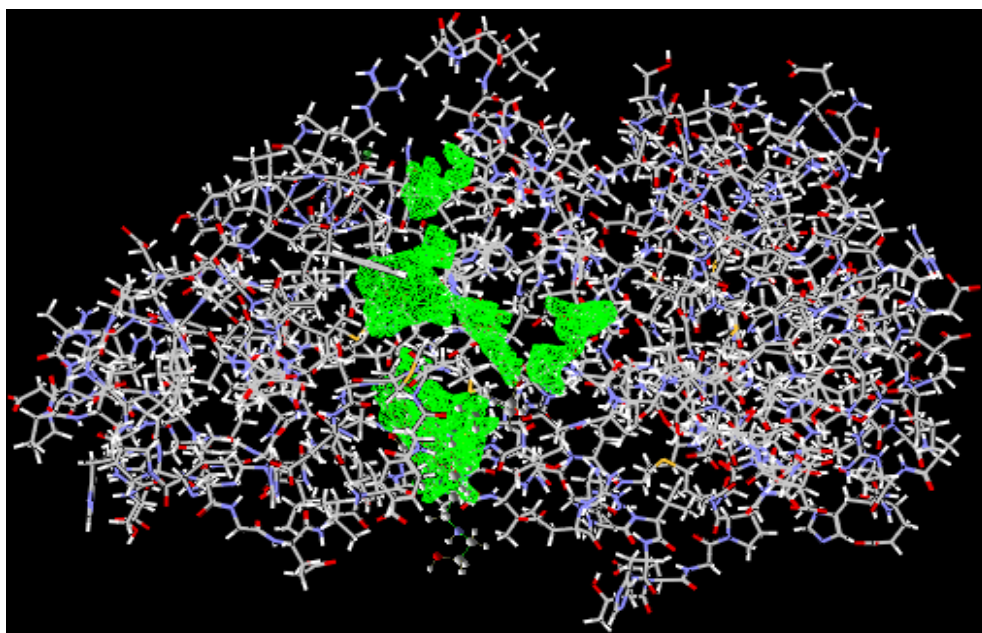


Fig.3. The five MVD- detected cavities in PknB, PDB code; 2FUM. Detected cavities; green; carbon atom; grey; oxygen atoms; red; nitrogen atoms; blue.

Protein-Ligand Docking

One application of molecular docking is to design pharmaceutical in *silico* by optimizing targeted lead candidates against protein. The lead candidates can be found using a docking algorithm that aims to identify the optimal binding mode of a small molecule (ligand) to the active site of macromolecular target. Ligands have been designed to obtain more potent compounds as inhibitors of PknB. Computational analysis was carried out on chain A of the enzyme 2FUM. The 29 ligands L1-29 were selected for the study of the protein-ligand interactions, five top poses for each ligand were returned in the simulation, out of which one best pose for each ligand was selected on the basis of their MolDock score. The MVD score and the re-ranks cores and H-Bound score (KJ/mol), for each docking studies of amino-pyrimidine ligands with 2FUM are summarized in (Table 2).

The docking of ligands outcome produced the three best ranked ligands, namely, L9, L12 and L21, which showed lower Moldock score, re-rank score and a higher number of hydrogen bonding interaction than the other compounds. The binding energy values of compounds L9, L12 and L21 are -161.475, -152.003 and -143.359 kcal/mol, respectively, which are better than MIX with binding energy value of -75.683 kcal/mol. These results show that, compared to MIX as selective PknB, those three top-ranked ligands will form more stable complex and selective with, as well as, be better able to inhibit and reduce the activity of PknB.

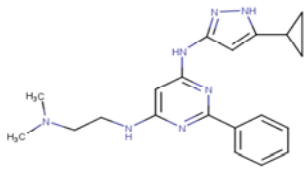
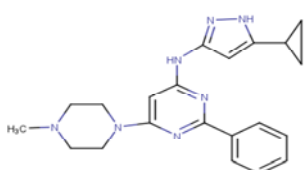
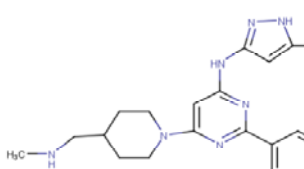
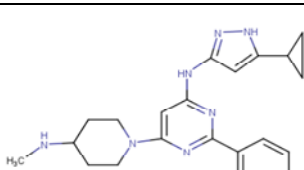
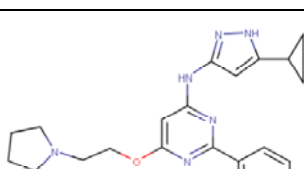
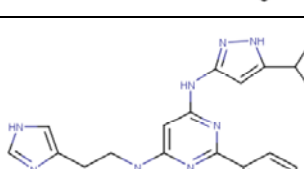
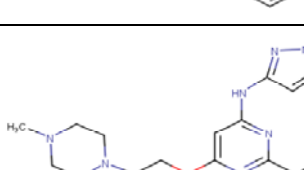
In addition, the docking results of the interactions between compounds to receptor can be analyzed by means of visualization using Molegro molecular viewer program. Visualization helps to observe amino acid residues contact and the hydrogen bonds formed between the ligand to the receptor. The number and length of hydrogen bonds the amino acid residues that interact with receptors of the compounds are shown in (Table 3) and (Figure 4).

The number of hydrogen bonds between ligands and amino acid of the target protein indicate its stability to inhibit the protein target.

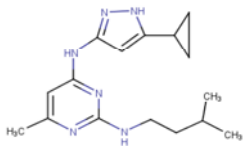
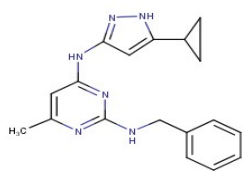
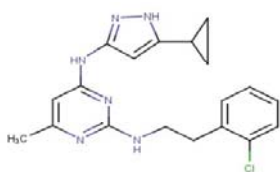
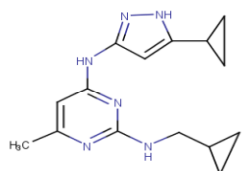
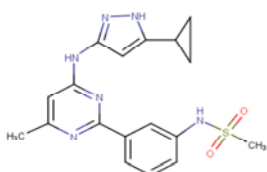
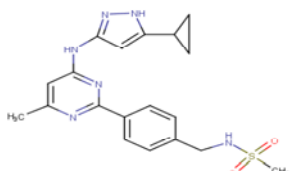
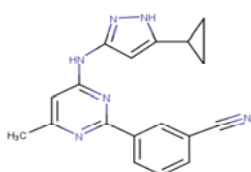
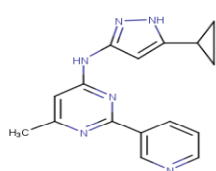
*Ligand 21, the most active ligand, formed six hydrogen bonds, and interacted with the Gly93, Val95, Lys140 and Asn143 active amino acid residues. Gly93 formed H-bonds with NH group of Pyrazole ring and Val 95 formed two hydrogen bonds with the N atom and the -NH group of Pyrazole ring, Lys140 forms two H-bonds with the two O (oxygen diatom) of the sulfonylmethane group and Asn143 formed H-bonds with the hydrogen atom of O

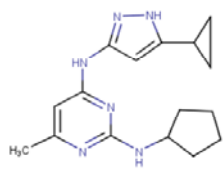
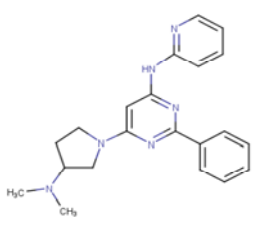
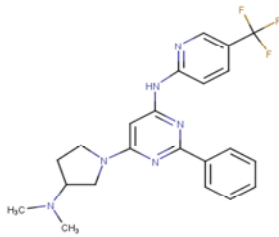
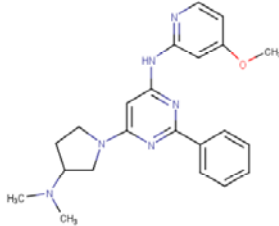
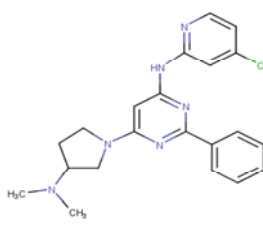
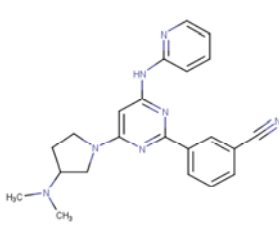
(oxygen diatom) of the sulfonyl group.

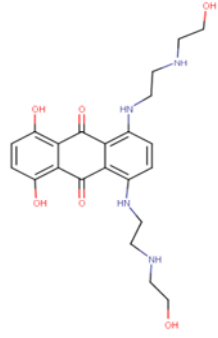
Table 2. The structure of amino-pyrimidine derivatives with docking scores.

| No | Ligand | Moldock score (KJ/mol) | Rerank score (KJ/mol) | H-Bound score (KJ/mol) |
|----|---|------------------------|-----------------------|------------------------|
| 1 |  | -147.646 | -69.264 | -2.276 |
| 2 |  | -144.615 | -95.918 | -2.014 |
| 3 |  | -139.421 | -116.664 | -6.416 |
| 4 |  | -139.71 | -29.120 | -5.586 |
| 5 |  | -155.848 | -96.502 | -7.761 |
| 6 |  | -147.347 | -109.939 | 0.0 |
| 7 |  | -155.794 | -120.147 | -2.618 |

| | | | | |
|----|--|----------|----------|--------|
| 8 | | -142.356 | -90.290 | -2.009 |
| 9 | | -161.475 | -128.826 | -7.237 |
| 10 | | -153.264 | -116.047 | -0.639 |
| 11 | | -151.906 | -119.35 | -2.961 |
| 12 | | -152.003 | -126.941 | -8.380 |
| 13 | | -123.111 | -99.842 | -4.821 |
| 14 | | -140.882 | -112.329 | -5.180 |
| 15 | | -133.398 | -105.768 | -4.163 |

| | | | | |
|----|---|----------|----------|--------|
| 16 |  | -127.542 | -94.644 | -2.693 |
| 17 |  | -134.871 | -96.723 | -2.636 |
| 18 |  | -135.756 | -100.839 | -7.316 |
| 19 |  | -125.914 | -95.786 | -7.169 |
| 20 |  | -143.71 | -112.077 | -5.767 |
| 21 |  | -143.359 | -120.853 | -9.685 |
| 22 |  | -133.614 | -107.115 | -4.613 |
| 23 |  | -120.633 | -99.877 | -5.483 |

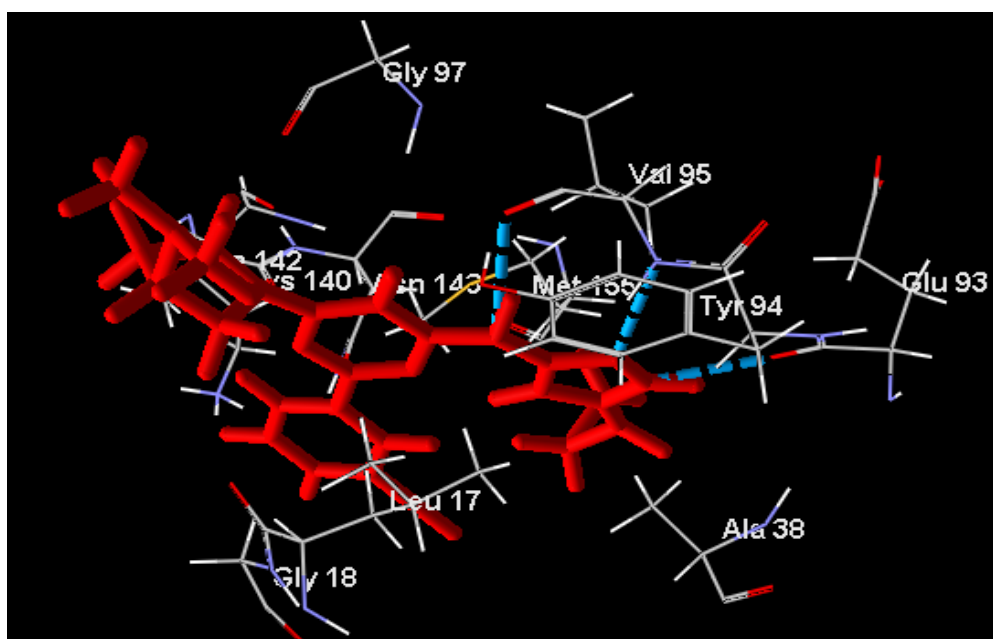
| | | | | |
|----|---|----------|----------|--------|
| 24 |  | -135.237 | -106.568 | -5.233 |
| 25 |  | -134.254 | -62.821 | -1.500 |
| 26 |  | -156.908 | -93359 | -1.364 |
| 27 |  | -170.109 | -94.358 | -3.122 |
| 28 |  | -138.238 | -111.629 | 0.0 |
| 29 |  | -136.307 | -108.308 | -2.035 |

| | | | | |
|-----|---|---------|---------|--------|
| MIX |  | -75.683 | -17.158 | -6.501 |
|-----|---|---------|---------|--------|

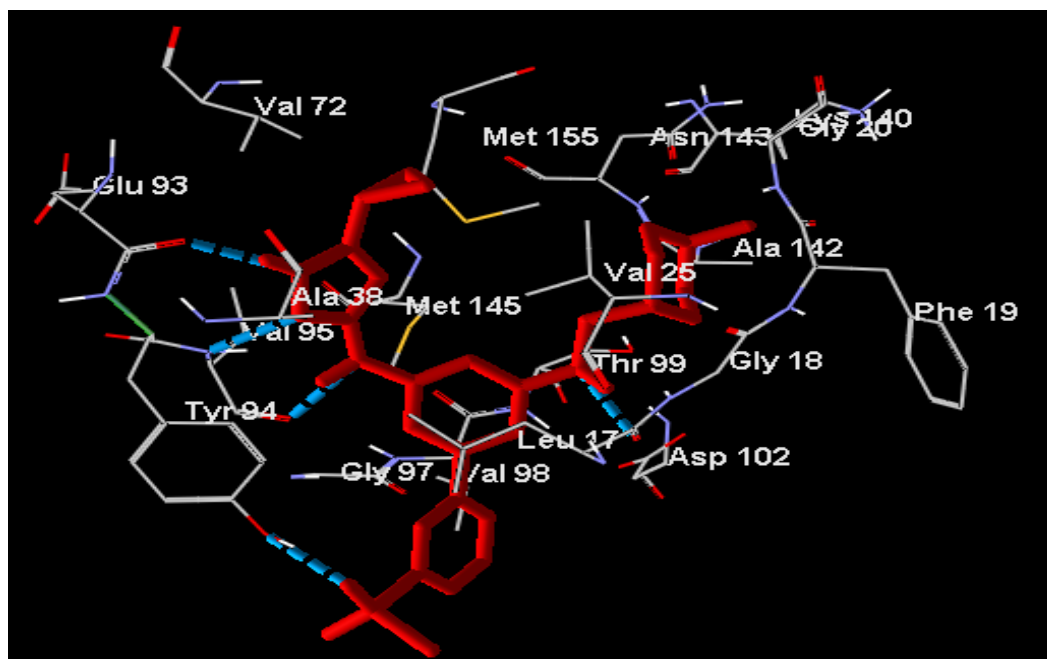
*Ligand 12 is the second most active ligand; it forms five hydrogen bonds, and interacted with the Gly93, Val95, Leu17 and Tyr 94 active amino acid residues. Gly93 formed H-bonds with NH group of pyrazole ring, whereas Val 95 formed two hydrogen bonds with the N atom and the -NH group of the pyrazole ring. Leu 17 and Tyr 94 formed respectively one H-bond with NH group and one H-bond with the H-bond atom of O (oxygen diatom) of the sulfonyl group.

*Ligand 9 is the less most active ligand; it forms three hydrogen bonds, and interacted with the Gly93 and Val95 active amino acid residues, respectively. Gly93 formed one H-bond with the NH group of pyrazole ring whereas Val 95 formed two hydrogen bonds with the N atom the -NH group of the pyrazole ring.

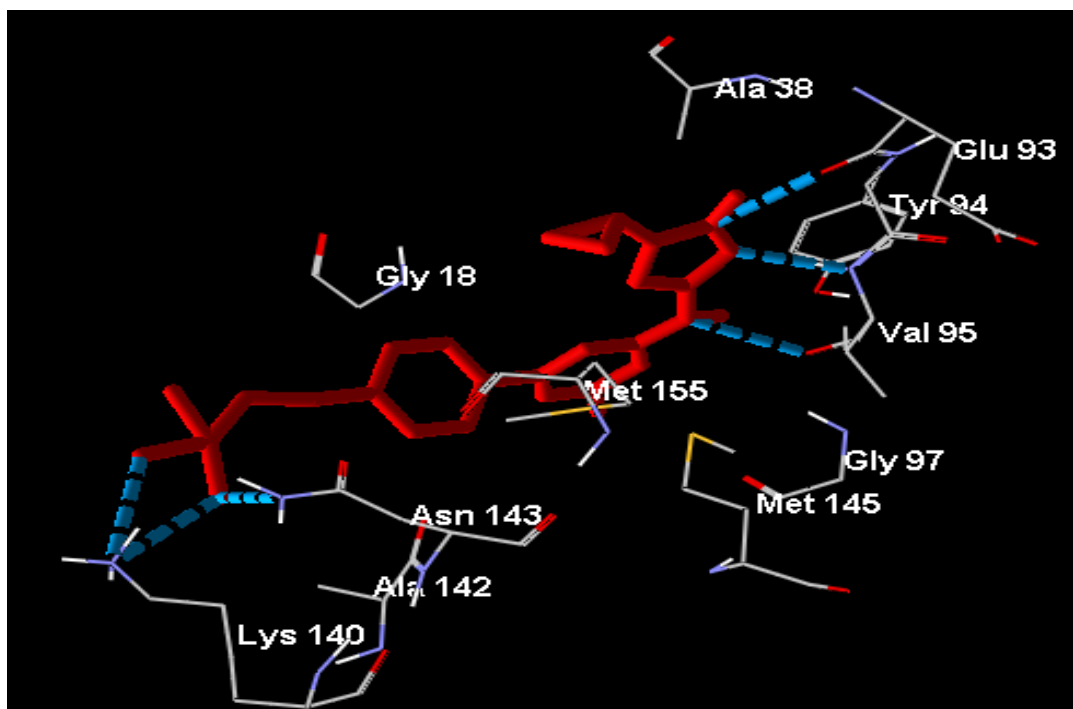
(A)



(B)



(C)



(D)

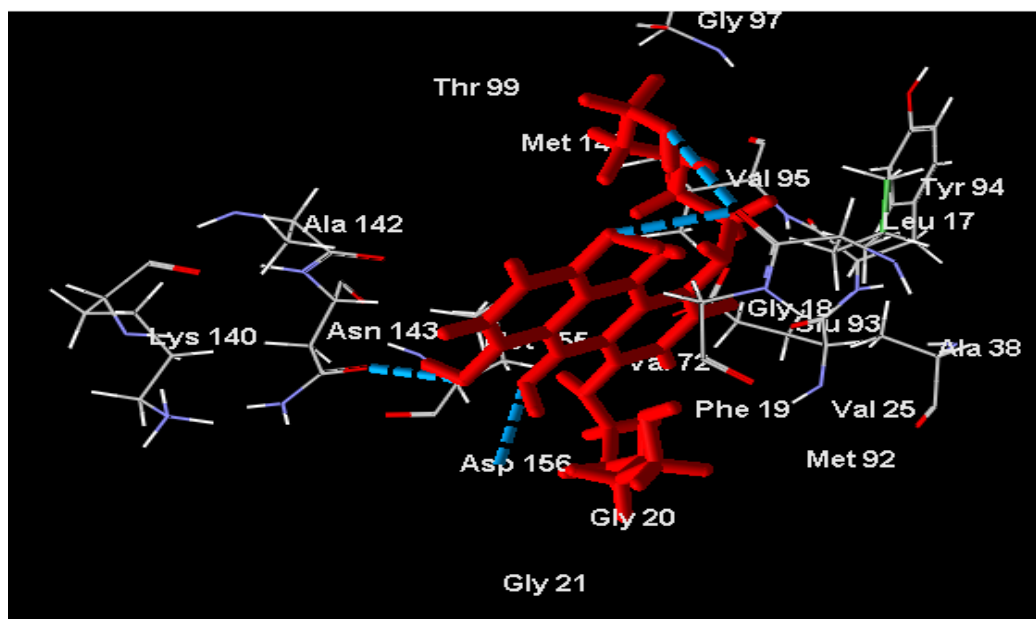


Fig.4.Hydrogen bonds interaction between ligands L9 (A), L12 (B), L21(C) and MIX(D) and residues of active site of 2FUM.

Table 3. Prediction interactions

| Compound | Ligand | | Annotated Distance | Protein | | | |
|----------|---------|---------|--------------------|------------------|---------|---------|---------|
| | Atom ID | Element | | Internal Residue | Atom ID | Residue | Element |
| L 9 | 0 | H | 2.60 | 90 | 691 | Gly93 | O |
| | 1 | N | 2.63 | 92 | 709 | Val95 | H |
| | 9 | H | 3.06 | 92 | 712 | Val95 | O |
| L 12 | 13 | H | 2.63 | 90 | 691 | Gly93 | O |
| | 14 | N | 2.61 | 92 | 709 | Val95 | H |
| | 9 | H | 2.69 | 92 | 712 | Val95 | O |
| | 22 | H | 2.83 | 14 | 116 | Leu17 | O |
| | 60 | O | 2.60 | 91 | 708 | Tyr94 | H |
| L 21 | 13 | H | 2.84 | 90 | 691 | Gly93 | O |
| | 12 | N | 2.73 | 92 | 709 | Val95 | H |
| | 9 | H | 3.12 | 92 | 712 | Val95 | O |
| | 45 | O | 3.15 | 137 | 1058 | Lys140 | H |
| | 43 | O | 3.23 | 137 | 1058 | Lys140 | H |
| | 43 | O | 3.16 | 140 | 1078 | Asn143 | H |

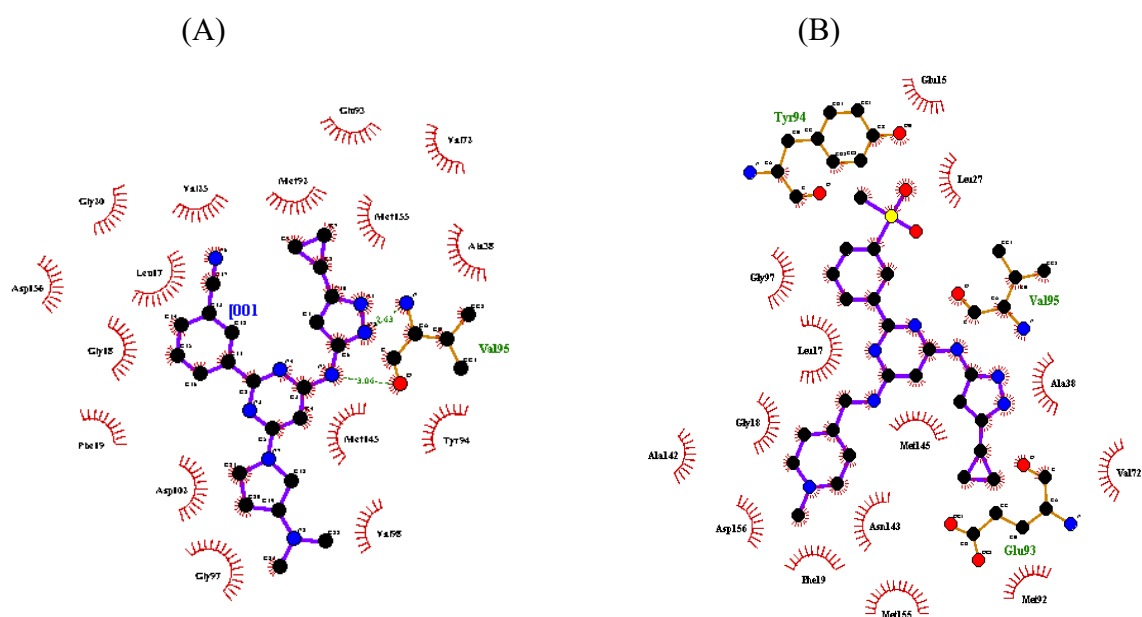
The lengths of the hydrogen bonds in the interval: $2.5\text{\AA} \leq x \leq 3.1\text{\AA}$ are considered strong interactions; however values in the interval $3.1\text{\AA} \leq x \leq 3.55\text{\AA}$: the averages interactions,

whereas values $> 3.55\text{\AA}$ are considered weak. It is noticed that the values obtained for distances of hydrogen bonds between the ligands L9, L12 and the residues of active site belong to the interval $2.5\text{\AA} \leq x \leq 3.1\text{\AA}$. These results indicate that the strong affinity of L9 and L12 on 2FUM could lead to the potent inhibition of the catalytic activity of the enzyme [44].

LigPlot is known as the comprehensive tool for expressing the hydrogen bonding and hydrophobic interactions involving the ligand molecule and active site residues

(Figure 4) gives a more detailed insight of the interactions with particular amino acids in enzyme binding pocket. Based on the presented results, it can be concluded that hydrophobic interactions between ligands L9, L12, L21 and binding pocket play an important role.

However, number, bond length and bond energy of hydrogen bonds formed between ligand and enzyme has an important role in ligand effect on investigated activity.



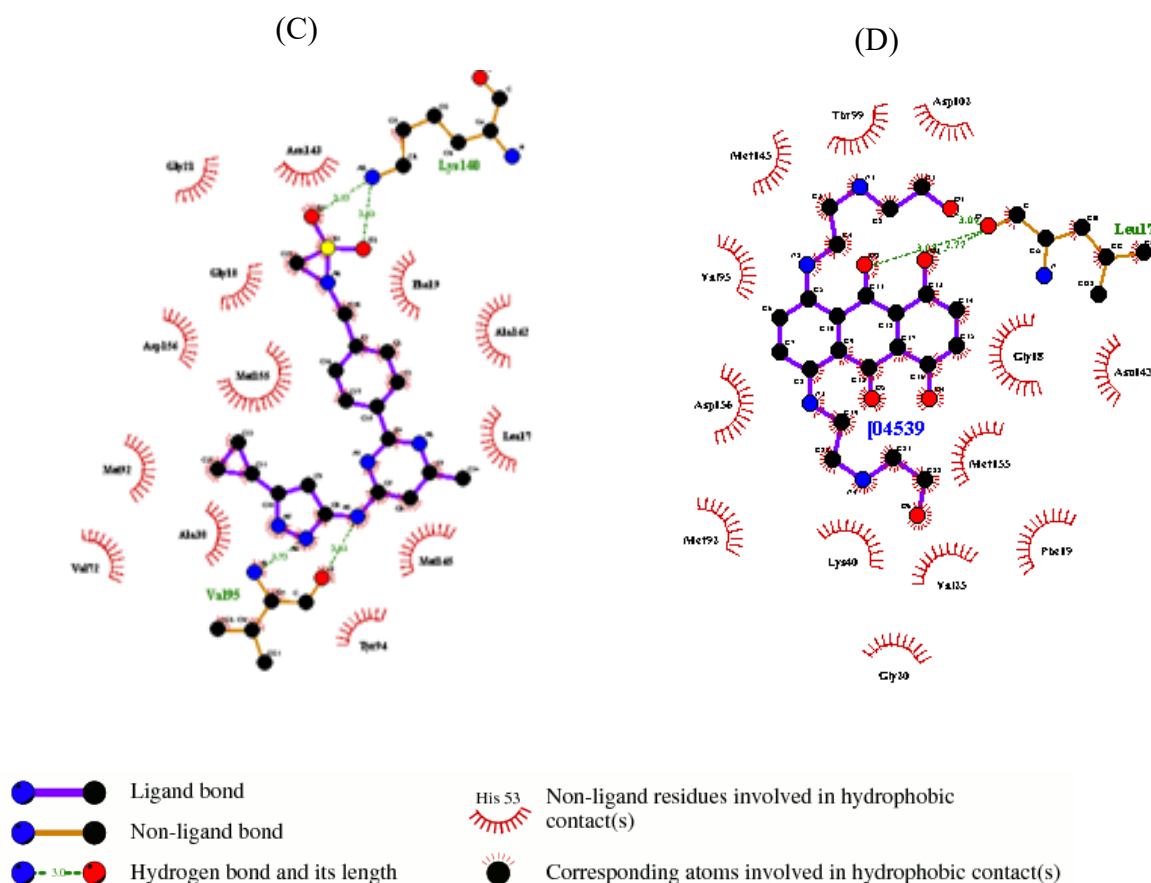


Fig.4. LigPlot generated for the best poses obtained with ligands L9 (A), L12 (B), L21 (C), MIX (D) and receptor 2FUM

Drug-likeness prediction of selected ligands

Physicochemical properties of selected ligands

The selected ligands used in this study were evaluated as selective inhibitor 2FUM protein target by comparison. The oral bioavailability of the compounds projected as potential drugs were evaluated by determining the molecular weight, number of rotatable bonds, H bond donor and acceptor, and drug's polar surface (TPSA). Since the individual molecular weights of all the compounds were less than 500, the numbers of the rotatable bond were < 10, the number of hydrogen bond donors and acceptors were < 10, an octanol-water partition coefficient $\log P$ not greater than 5.

TPSA values being <140, they qualified to be an ideal oral drug. Ligands tested in this study were also predicted to have good oral bioavailability and all the ligand qualify of the Lipinski's Rule of 5.

According to (Table 4), all the ligands possess limited aqueous solubility which ranged from very slightly soluble to practically insoluble [45]. This result is also supported by the calculation of partition coefficient which indicates that all the tested compounds are lipophilic and have the best affinity to reside in *n*-octanol than in water i.e. all the ligands will pass the plasma membrane easily (Table 4)

Table 4. Physicochemical property of anti-tubercular ligands.

| Ligand | Molecular weight | Intrinsic aqueous solubility logS | Partition coefficient (logP) | | H bond donor | H bond acceptor | TPSA |
|--------|------------------|-----------------------------------|------------------------------|----------|--------------|-----------------|--------|
| | | | Consensus | ChemAxon | | | |
| L9 | 414.517 | -5.95 | 4.46 | 4.81 | 2 | 8 | 96.76 |
| L12 | 481.62 | -4.87 | 3.32 | 3.55 | 3 | 9 | 115.90 |
| L21 | 398.49 | -4.65 | 2.66 | 2.88 | 3 | 8 | 112.66 |

In drug-likeness prediction, a molecule can be considered to have drug-like features Only if it satisfies most of the rules including rule of five, CMC-like rule, MDDR-like rule, Lead-like rule, WDI-like rule. All of the selected ligands qualified Lipinski's rule, WDI rule as it was in the cut-off range (90%) and CMC-like rule expected L12 and MIX, such as MIXMDDR rule, whereas L9, L12, L21 showed mid-structure to MDDR-like rule. However, all ligands Violated Lead-like rule (Table 5).

Table 5. Drug likeness prediction using PreADMET Server

| Ligands | CMC like rule | Lead like rule | Lipinski's "Rule of five" | WDI like rule | MDDR Like |
|---------|---------------|----------------|---------------------------|---------------|---------------|
| L9 | Qualified | Violated | Suitable | Out of 90 % | Mid-structure |
| L12 | Not Qualified | Violated | Suitable | Out of 90 % | Mid-structure |
| L21 | Qualified | Violated | Suitable | Out of 90 % | Mid-structure |
| MIX | Not Qualified | Violated | Suitable | Out of 90 % | Drug-like |

Pharmacokinetic study of selected ligands

The pharmacokinetic studies such as absorption, distribution of L9, L12, L21 and MIX were performed using online server PreADMET (<https://preadmet.bmdrc.kr/>). The calculated

absorption, distribution parameters are presented in (Table 6).

The calculated human intestinal absorption (HIA) was ranged from 85.48% to 90.926 % which suggest that all the tested compounds are well absorbed through the intestinal cell [46].

Table 6.ADME properties of ligands

| Ligands | Absorption | | | Distribution | | |
|---------|--------------------------------------|--|-------------------|----------------------------|---|-----------------------------|
| | Human intestinal Absorption (HIA, %) | In vitro Caco-2 cell permeability (nm/s) | Skin permeability | plasma Protein binding (%) | blood brain barrier penetration (c.brain/c.blood) | P-Glycoprotein (Inhibition) |
| L9 | 90.926 | 15.148 | -3.721 | 82.193 | 1.141 | Inhibitor |
| L12 | 89.806 | 1.605 | -2.642 | 87.243 | 0.292 | Inhibitor |
| L21 | 85.480 | 6.312 | -2.704 | 93.097 | 0.118 | Non inhibitor |
| MIX | 22.314 | 18.258 | -5.094 | 22.314 | 0.029 | Non inhibitor |

In addition, all compounds exhibited high permeability [47] as absorption values through Caco-2 cell (PCaco-2) were within 15.148 - 6.312 nm/s excepted l9 (1.605 nm/s) The skin permeability (PSkin) is a vital parameter for the assessment of drugs and chemical that might require trans dermal administration. All the compounds were found to be impermeable through skin since the calculated PSkin value was negative.

The distribution properties were assessed by evaluating the brain to blood partition coefficient (Cbrain/Cblood), plasma binding (PPB) and interaction with the P-glycoprotein (Pgp). The calculated values of PPB were 82.193 to 93.097 %. Generally compounds with more than 90% of PPB are classified as strongly bound chemicals whereas less than 90% are weakly bound chemicals (<https://preadmet.bmdrc.kr/adme-prediction/>). Therefore, among L21 bound

strongly with plasma protein whereas L9 and L12 are weakly bound chemicals. The C_{brain}/C_{blood} values were 0.118 to 1.141. Based on C_{brain}/C_{blood} ratio all chemicals fall under three categories namely high absorption to CNS (C_{brain}/C_{blood} value more than 2.0), middle absorption to CNS (C_{brain}/C_{blood} value within 2.0 - 0.1) and low absorption to CNS (C_{brain}/C_{blood} value less than 0.1). The ratio of C_{brain}/C_{blood} suggests middle absorption of these agents to CNS indicating moderate to higher ability to cross blood brain barrier (BBB). P-glycoprotein (Pgp), produced from the multi drug resistance (MDR) gene and an ATP dependent efflux transporter that affects the absorption, distribution and excretion of clinically important drugs [48].

The ligands L9 and L12 are inhibitors for Pgp and L12 but are not inhibitors for Pgp.

Ligand L21 showed PPB=93.097%, HIA= 85.48 and C_{Brain}/C_{Blood}=6.312, this ligand will be with greater availability to bind with the target receptor, showing pharmacological effect for possessing a lower penetration of the blood-brain barrier, causing less collateral effects when compared to other compounds.

Toxicological study of selected ligands

Table 5 shows the results of mutagenic (Ames test) and carcinogenic (using mouse and rat model) properties of L9, L12, L21 and MIX. Toxicological investigation of drug candidates is one of the key steps for drug discovery. This means that the toxicity study is very important for new compounds.

The Ames test is widely used and an accepted test to evaluate the mutagenicity of a chemical agent. In this test, all the compounds except L12, L21 exhibited positive prediction mutagenic compound.

Table 7. Toxicological properties of anti-tubercular agents.

| Ligands | Mutagenicity (Ames test) | Carcinogenicity | | in vitro hERG inhibition |
|---------|--------------------------|-----------------|----------|--------------------------|
| | | Mouse | Rat | |
| L9 | mutagen | Negative | Negative | Medium risk |
| L12 | non-mutagen | Negative | Negative | Ambiguous |
| L21 | non-mutagen | Negative | Negative | Ambiguous |

| | | | | |
|-----|-------------|----------|----------|-----------|
| | | | | |
| MIX | non-mutagen | Negative | Negative | Ambiguous |

In carcinogenicity study, the PreADMET server was utilized to predict the carcinogenicity of chemical agent.

In the prediction of carcinogenicity, negative prediction indicates there is evidence of carcinogenic activity whereas positive means the tested compound does not exhibit carcinogenic activity. Among all ligands demonstrated carcinogenicity in both mouse and rat model. The risk of inhibition of human ether-a-go-go-related (hERG) gene was varied from medium and ambiguous. Inhibition of the hERG gene has been linked to long QT syndrome. The results have been summarized in (Table 7).

4. CONCLUSION

Virtual screening methods are widely used for reducing cost and time of drug discovery process. From this study of *in silico* drug designing and molecular docking of the 29 amino-pyrimidine derivatives, we conclude that those derivatives have the ability to inhibit the Mycobacterium tuberculosis protein kinase B. The scoring results reveal the higher negative mol dock score, rerank score and hydrogen bond interaction of the title compounds in comparison to MIX. It was found that the three ligands L9, L12, L21 showed better results from 29 docked ligands. Furthermore, Pharmacokinetic effects of the ligand L21 observed comparatively better bioavailability, distribution, absorption, than MIX and other ligands. Hence, it could be concluded that the ligand L21 could be considered as potent drug candidate of M. tuberculosis.

5. REFERENCES

- [1] McDonough K A, Kress Y, Bloom B R, Pathogenesis of tuberculosis: interaction of Mycobacterium tuberculosis with macrophages. Infect Immun., 1993, 61 (7), 2763–2773.
- [2] Rohini K , Srikumar P S, Insights from the docking and molecular dynamicssimulation of the Phosphopantetheinyl transferase (PptT) structural model from Mycobacterium tuberculosis,

Bioinformatics, 2013, 9 (13), 685–689. doi: 10.6026/97320630009685

[3] Loughheed K E A, Osborne S A, Saxty B, Whalley D, Chapman TM, Bouloc N, Chugh J, Nott T J, Patel D, Spivey V L, Kettleborough C A, Bryans J S, Taylor D L, Smerdon S J and Buxton R S. Effective inhibitors of the essential kinase PknB and their potential as anti-mycobacterial agents. *Tuberculosis (Edinb)*, 2011, 91 (4), 277–286. doi: 10.1016/j.tube.2011.03.005

[4] Gorakh W J, Sachan S, Ahuja D, and Angshu B. Designing of potential drug-like inhibitors to serine-threonine protein kinase b (pknb) in tuberculosis through computer-aided drug design *World. J. Pharm. Res.*, 2014,3(2),3945-3974.

[5] Khamouli S, Belaidi S, Belaidi H, Belkhiri L, QSAR Studies of amino-pyrimidine derivatives as *Mycobacterium tuberculosis* Protein Kinase B inhibitors. *Turkish Comp. Theo. Chem. (TC&TC)*., 2018,2(2), 16 – 27. doi: 10.33435/tcandtc.397449

[6] Barthe P, Mukamolova G V, Roumestand C, and Cohen-Gonsaud M. The Structure of PknB Extracellular PASTA Domain from *Mycobacterium tuberculosis* Suggests a Ligand-Dependent Kinase Activation. *Structure*, 2010, 18 (5), 606–615. doi.org/10.1016/j.str.2010.02.013

[7] Young T A, Delagoutte B, Endrizzi J A, Falick A M, and Alber T. Structure of *Mycobacterium tuberculosis* PknB supports a universal activation mechanism for Ser/Thr protein kinases. *Nat. Struct. Biol.*, 2003,105(3), 168–174. doi:10.1038/nsb897

[8] Av-Gay Y, Jamil S, and Drews S J. Expression and characterization of the *Mycobacterium tuberculosis* serine/threonine protein kinase PknB. *Infect. Immun.*, 1999, 67, (11), 5676–5682.

[9] Fernandez P et al.. The Ser/Thr Protein Kinase PknB Is Essential for Sustaining *Mycobacterial* Growth. *J. Bacteriol.*, 2006,188(22), 7778–7784. doi: 10.1128/JB.00963-06

[10] Mieczkowski C, Iavarone AT, and Alber T. Auto-activation mechanism of the *Mycobacterium tuberculosis* PknB receptor Ser/Thr kinase. *EMBO J.*, 2008, 27(23), 3186–3197. doi: 10.1038/emboj.2008.236.

[11] Sharma K, Gupta M, Krupa A, Srinivasan N, and Singh Y. EmbR a regulatory protein with ATPase activity, is a substrate of multiple serine/threonine kinases and phosphatase in *Mycobacterium*. *FEBS J.*, 2006, 273 (12), 2711–2721. doi.org/10.1111/j.1742-4658.2006.05289.x

-
- [12] Dasgupta A, Datta P, Kundu M, and Basu J. The serine/threonine kinase PknB of *Mycobacterium tuberculosis* phosphorylates PBPA, a penicillin-binding protein required for cell division. *Microbiology*, 2006, 152, 493-504. doi:10.1099/mic.0.28630-0.
- [13] Kang CM, Abbott D W, Park S T, Dascher C C, Cantley L C, and Husson R N. The *Mycobacterium tuberculosis* serine/threonine kinases PknA and PknB: substrate identification and regulation of cell shape. *Genes Dev.*, 2005, 19(14), 1692–1704. doi :10.1101/gad.1311105
- [14] Ortiz-Lombardía M, Pompeo F, Boitel B, and Alzari P M. Crystal structure of the catalytic domain of the PknB serine/threonine kinase from *Mycobacterium tuberculosis*. *J. Biol. Chem.*, 2003, 278(15), pp. 13094–13100. doi:10.1074/jbc.M300660200
- [15] Narayan A, Sachdeva P, Sharma K, Saini AK, Tyagi AK, and Singh Y. Serine threonine protein kinases of mycobacterial genus: phylogeny to function. *Physiol Genomics.*, 2007, 29 (1), 66–75. doi :10.1152/physiolgenomics.00221.2006
- [16] Villarino A et al. Proteomic identification of *M. tuberculosis* protein kinase substrates: PknB recruits GarA, a FHA domain-containing protein, through activation loop-mediated interactions. *J. Mol. Biol.*, 2005, 350(5), 953–963. doi:10.1016/j.jmb.2005.05.049
- [17] Chapman T M, Bouloc N, Buxton R S, Chugh J, Lougheed K E A, Osborne S A, Saxty B, Smerdon S J, Taylor D L and Whalley D. Substituted aminopyrimidine protein kinase B (PknB) inhibitors show activity against *Mycobacterium tuberculosis*, *Bioorg .Med .Chem. Lett.*, 2012, 22 (9), 3349–3353. doi: 10.1016/j.bmcl.2012.02.107
- [18] Seal A, Yogeeswari P, Sriram D, Consortium O, and Wild D J. Enhanced ranking of PknB Inhibitors using data fusion methods. *Journal of Cheminformatics*, 2013, 5 (1), 1-11. Jan. 2013. doi:10.1186/1758-2946-5-2
- [19] Székely R et al. A novel drug discovery concept for tuberculosis: inhibition of bacterial and host cell signalling. *Immunol. Lett.*, 2008, 116 (2), 225–231. doi.org/10.1016/j.imlet.2007.12.005
- [20] Hegymegi-Barakonyi B et al. Signalling inhibitors against *Mycobacterium tuberculosis*--early days of a new therapeutic concept in tuberculosis. *Curr. Med. Chem.*, 2008, 15 (26), 2760–2770.

-
- [21] Wehenkel A et al. The structure of PknB in complex with mitoxantrone, an ATP-competitive inhibitor, suggests a mode of protein kinase regulation in mycobacteria. *FEBS Lett.*, 2006,580(13),3018–3022. doi: 10.1016/j.febslet.2006.04.046
- [22] Khamouli S, Belaidi S, Almi Z, Medjahed S, and Belaidi H. Property/Activity Relationships and Drug Likeness for Pyrimidine Derivatives as Serine/Threonine Protein Kinase B Inhibitors. *J. Bionanosci.*, 2017,11(4),301–309. doi.org/10.1166/jbns.2017.1445.
- [23] Lyskov S and Gray J J. The Rosetta Dock server for local protein–protein docking. *Nucleic Acids Res.*, 2008, 36(2), 233–238. doi:10.1093/nar/gkn216
- [24] Ouassaf M, Belaidi S, Lotfy K, Daoud I, and Belaidi H. Molecular Docking Studies and ADMET Properties of New 1.2.3 Triazole Derivatives for Anti-Breast Cancer Activity. *J. Bionanosci.*, 2018, 12,1-11. doi:10.1166/jbns.2018.1505
- [25] 2FUM: 3-dimensional structure downloaded from <http://www.rcsb.org/pdb>.
- [26] Wehenkel A et al. The structure of PknB in complex with mitoxantrone, an ATP-competitive inhibitor, suggests a mode of protein kinase regulation in mycobacteria. *FEBS Lett.*, 2006,580(13), 3018–3022. doi:10.1016/j.febslet.2006.04.046.
- [27] Ramachandran G N, Ramakrishnan C, and Sasisekharan V . Stereochemistry of polypeptide chain configurations. *J. Mol. Biol.*, 1963,7, 95–99.
- [28] Damre M V , Gangwal R P, Dhoke G V, Lalit M, Sharma D, Khandelwal K, and Sangamwar A T. 3D-QSAR and molecular docking studies of amino-pyrimidine derivatives as PknB inhibitors. *J. Taiwan Inst. Chem. Eng.*, 2014, 45 (2), 354–364 doi.org/10.1016/j.jtice.2013.05.016
- [29] Hyper Chem (Molecular Modeling System) Hypercube, Inc., 1115 NW, 4th Street, Gainesville, FL 32601, USA.2008.
- [30] MarvinSketch 17.1.2, Chemaxon .2017, (<http://www.chemaxon.com>).
- [31] <http://molegro.com/mvd-product.php>
- [32] Bursulaya B D, Totrov M, Abagyan R, and Brooks C L .Comparative study of several algorithms for flexible ligand docking. *J. Comput. Aided Mol. Des.*, 2003, 17(11), 755–763
- [33] Thomsen R , Christensen M H. MolDock: A New Technique for High-Accuracy Molecular Docking. *J. Med. Chem.*, 2006, 49 (11), 3315–3321. doi:10.1021/jm051197e

-
- [34] Anuf A R, Ramaraj K. Inhibition of FGFR2 signal transduction in Acne Vulgaris using Bioactive Flavonoids: An Insilico approach . J .Med. Pharm. Sci., 2014, 2(2), 136–142.
- [35] Wallace A C, Laskowski R A, and Thornton J M. LIGPLOT: a program to generate schematic diagrams of protein-ligand interactions. Protein Eng., 1995, 8(2), 127–134
- [36] Veber D F, Johnson S R, Cheng H Y, Smith B R, Ward KW, and Kopple K D, Molecular properties that influence the oral bioavailability of drug candidates. J. Med. Chem., 2002 45(12), 2615-2623.
- [37] Lipinski C A, Lombardo F, Dominy B W, and Feeney P J. Experimental and computational approaches to estimate solubility and permeability in drug discovery and development settings. J. Adv. Drug Deliv. Rev., 2001, 46(1-3), 3-26.
- [38] Ajay A, Walters W P, and Murcko M A. Can We Learn To Distinguish between ‘Drug-like’ and ‘Nondrug-like’ Molecules?. J. Med. Chem., 1998, 41 (18), 3314–3324.
doi :10.1021/jm970666c
- [39] Oprea T I, Allu T K, Fara D C, Rad R F, Ostopovici L, and Bologa C G . Lead-like, Drug-like or ‘Pub-like’: How different are they?. J Comput Aided Mol Des., 2007, 21(1–3), 113–119. doi:10.1007/s10822-007-9105-3
- [40] Wagener M , Van Geerestein V J .Potential Drugs and Nondrugs: Prediction and Identification of Important Structural Features . J. Chem. Inf. Comput. Sci., 2000, 40(2), 280–292. doi: 10.1021/ci990266t
- [41] Kulkarni A, Han Y, and Hopfinger A J. Predicting Caco-2 Cell Permeation Coefficients of Organic Molecules Using Membrane-Interaction QSAR Analysis. J. Chem. Inf. Comput. Sci., 2002, 42(2), 331–342. doi: 10.1021/ci010108d
- [42] Irvine J D et al. MDCK (Madin-Darby canine kidney) cells: A tool for membrane permeability screening. J Pharm Sci, vol. 88, no. 1, pp. 28–33, Jan. 1999.
doi:10.1021/js9803205
- [43] Lovell S C et al. Structure validation by C α geometry: phi, psi and C β deviation. Proteins, 2003, 50(3), 437–450.

- [44] Imberty A, Hardman K D, Carver J P, and Pérez S. Molecular modeling of protein-carbohydrate interactions. Docking of monosaccharides in the binding site of concanavalin A. *Glycobiology*, 1991,1(6), 631–642.
- [45] Sinko P J. *Martin's Physical Pharmacy and Pharmaceutical Sciences: Physical Chemical and Biopharmaceutical Principles in the Pharmaceutical Sciences*, 6th Edition, Lippincott.2010, pp 183.
- [46] Yee S. In vitro permeability across Caco-2 cells (colonic) can predict in vivo (small intestinal) absorption in man--fact or myth. *Pharm. Res.*, 1997, vol. 14(6), 763–766.
- [47] Yazdanian M, Glynn S L, Wright J L, and Hawi A. Correlating partitioning and caco-2 cell permeability of structurally diverse small molecular weight compounds. *Pharm. Res.*, 1998, 15 (9),1490–1494.
- [48] Schinkel A H. P-Glycoprotein, a gatekeeper in the blood-brain barrier.*Adv. Drug Deliv. Rev.*,1999, 36 (2–3), 179–194, Apr. 1999.

How to cite this article:

Khamouli S, Belaidi S, Lanez T. Molecular doking and admet studies of amino-pyrimidine derivaties as mycobacterium tuberculosis ser/thr protein kinases b inhibitors. *J. Fundam. Appl. Sci.*, 2019, 11(2), 914-939.